

**BUDAPEST UNIVERSITY OF TECHNOLOGY  
AND ECONOMICS**

**Politecnico di Milano**

Multi-scale Topology Optimization With  
Graded Microstructures

by

Hussein Ismail

2024

Supervised by:

**Prof. János Lógó - BME**

**Prof. Matteo Bruggi - POLIMI**

A Summary

# Contents

|          |   |           |
|----------|---|-----------|
| <b>1</b> | <b>Introduction</b>   | <b>1</b>  |
| 1.1      | History of Topology Optimization . . . . .  | 2         |
| 1.2      | Multiscale Topology Optimization in Additive Manufacturing . . . . .              | 3         |
| 1.3      | Overview of Topology Optimization Under Uncertainty . . . . .                     | 4         |
| 1.4      | Software Utilized in Our Research . . . . .                                       | 4         |
| <b>2</b> | <b>Topology Optimization for Loads with Multiple Points of Application</b>        | <b>5</b>  |
| 2.1      | Problem Statement . . . . .   | 5         |
| 2.2      | Numerical Implementation . . . . .  | 6         |
| 2.3      | Results . . . . .   | 7         |
| 2.4      | Conclusions . . . . .   | 8         |
| <b>3</b> | <b>Lightweight Additive Design: Graded Porosity with Displacement Constraints</b> | <b>9</b>  |
| 3.1      | A Two-Phase Material Model with Void . . . . .                                    | 9         |
| 3.2      | Formulation . . . . .   | 11        |
| 3.3      | Post-Processing for Manufacturing . . . . .                                       | 12        |
| 3.4      | Results . . . . .   | 13        |
| 3.5      | Conclusions . . . . .   | 15        |
| <b>4</b> | <b>Topology Optimization with Graded Infill for Loading Uncertainty</b>           | <b>16</b> |
| 4.1      | Material Law . . . . .  | 16        |
| 4.2      | Probabilistic Formulation . . . . .   | 17        |
| 4.3      | Results . . . . .   | 19        |
| 4.4      | Conclusions . . . . .   | 21        |
| <b>5</b> | <b>New Scientific Results</b>   | <b>22</b> |
| 5.1      | Theses 1 . . . . .  | 22        |
| 5.2      | Theses 2 . . . . .  | 22        |
| 5.3      | Theses 3 . . . . .  | 23        |
| 5.4      | List of Publications . . . . .  | 23        |
|          | <b>Bibliography</b>   | <b>25</b> |

## Chapter 1

# Introduction

The dissertation focuses on optimizing lightweight structural components using a multi-scale topology optimization framework, addressing challenges with graded infills and displacement constraints. It employs an augmented Lagrangian method based on advancements in stress-based optimization to solve multi-constrained volume problems. The analysis includes structural performance of 2D/3D microstructures with hexagonal arrangements of holes, utilizing numerical homogenization for deriving elastic properties for lightweight infills. The design process two-material structures, made by a full phase and a graded one, along with void, is refined using suitable interpolation laws. The study delves into the design of composite structures not only by considering deterministic loads, but also by providing a focus on the impact of uncertainties that may affect the loading amplitude. The findings highlight the effectiveness and the numerical efficiency of the proposed approaches in optimizing lightweight structural components composed by a solid phase and an infill one. The achieved composite layouts leverage on the potential of additive manufacturing in creating complex porous layouts to gain stiffness and redundancy of the load path, and to avoid the overhang problems.

Following this summary of the dissertation's core contributions, the subsequent sections are organized into three main topics that further elaborate on the methodologies and applications explored.

In the first topic, a topology optimization formulation was developed to minimize the volume of structures while adhering to multiple displacement constraints. This approach utilized a modified Augmented Lagrangian method integrated with sequential convex programming to handle the complexities of multi-constraint optimization and to accommodate both fixed and varying loads. Additionally, two deflection enforcement strategies were assessed: a uniform upper bound typical for serviceability limit states and a variable limit that mimics the stiffness of a fully materialized beam, both significantly influencing the optimization outcomes.

In the second topic, a multi-scale topology optimization method was introduced, using numerical homogenization to assess the properties of porous materials and implementing a mixed-material approach for optimal density distribution. This method incorporated hexagonal close-packed arrangements of circular or spherical holes to define isotropic or transversely isotropic microstructures in both 2D and 3D. The process allowed for the

clear identification of solid and graded regions, included discussions on post-processing techniques for defining component boundaries and internal structures, and facilitated the creation of coated structures adaptable to various loads.

In the third topic, a numerical method of homogenization-based topology optimization was proposed to account for uncertainty in loading amplitude, transforming stochastic displacement constraints into deterministic enforcements. This method enabled the design of minimum weight structures with specified probabilities for exceeding displacement limits. Moreover, macroscopic elastic constants of isotropic and orthotropic infills commonly used in additive manufacturing were derived, a two-phase material law was adopted, and it was demonstrated that the type of lattice grading significantly affects the topology and structural performance under load uncertainties.

## Section 1.1 History of Topology Optimization

The field of structural optimization, particularly topology optimization, has been a focal point of engineering research for approximately 150 years. Early progress in this area, once obscured by secrecy, saw significant contributions from researchers at renowned institutions like Cambridge and Oxford Universities during the 1950s. The advent of digitalization in the post-1970s era transformed the field, dramatically enhancing the accessibility and documentation of research. This shift greatly improved the distribution of knowledge within the optimization community, marking the evolution of topology optimization from a niche academic area to a well-established and extensively documented field of study.

In the second half of the 20<sup>th</sup> century, a significant number of structural optimization problems were addressed using what is known in the literature as optimality criteria methods. These methods depart fundamentally from the mathematical programming methods developed during the same period. Whereas mathematical programming methods focus on iterative improvements at the current design point in design space, exploring direction and magnitude changes to minimize the objective function, optimality criteria methods establish or derive conditions characterizing the optimal design and adjust the design to satisfy these conditions, thus optimizing the structure indirectly. The classical optimality criteria method originated in the 1970s emphasizes stiffness-related constraints and utilizes classical Lagrangian multiplier methods to derive theoretically valid optimality criteria for discretized structures. Berke [6], and later Berke and Khot [7], proposed an algorithm based on this approach. This algorithm provided an exact direct formula for statically determinate structures and was designed to converge quickly for most practical structures. The classical optimality criteria method is theoretically applicable to indeterminate structures, and it also allows for the separability of variables, enabling member-by-member resizing. Berke further suggested that design variables and constraints be separated into a passive and active set, drawing parallels between the terminology and procedural steps of the classical optimality criteria method and the Solid Isotropic Material with Penalization (SIMP) method, one of the leading solution procedures in contemporary topology

optimization.

## Section 1.2 Multiscale Topology Optimization in Additive Manufacturing

Additive manufacturing has become increasingly relevant as a competitive alternative to traditional subtractive manufacturing, particularly due to its flexibility in creating customized products through 3D printing and topology optimization. Lattice structures, which can be manufactured easily via 3D printing, offer lightweight, robust, and multifunctional infills. The design of optimal infills and external shapes are facilitated through topology optimization, with multi-scale topology optimization being a notably effective technique as reviewed in [22]. Numerical homogenization is used at different scales to compute the effective elastic properties of lattice materials, incorporating geometric parameters to optimize microstructure within the design domain [23].

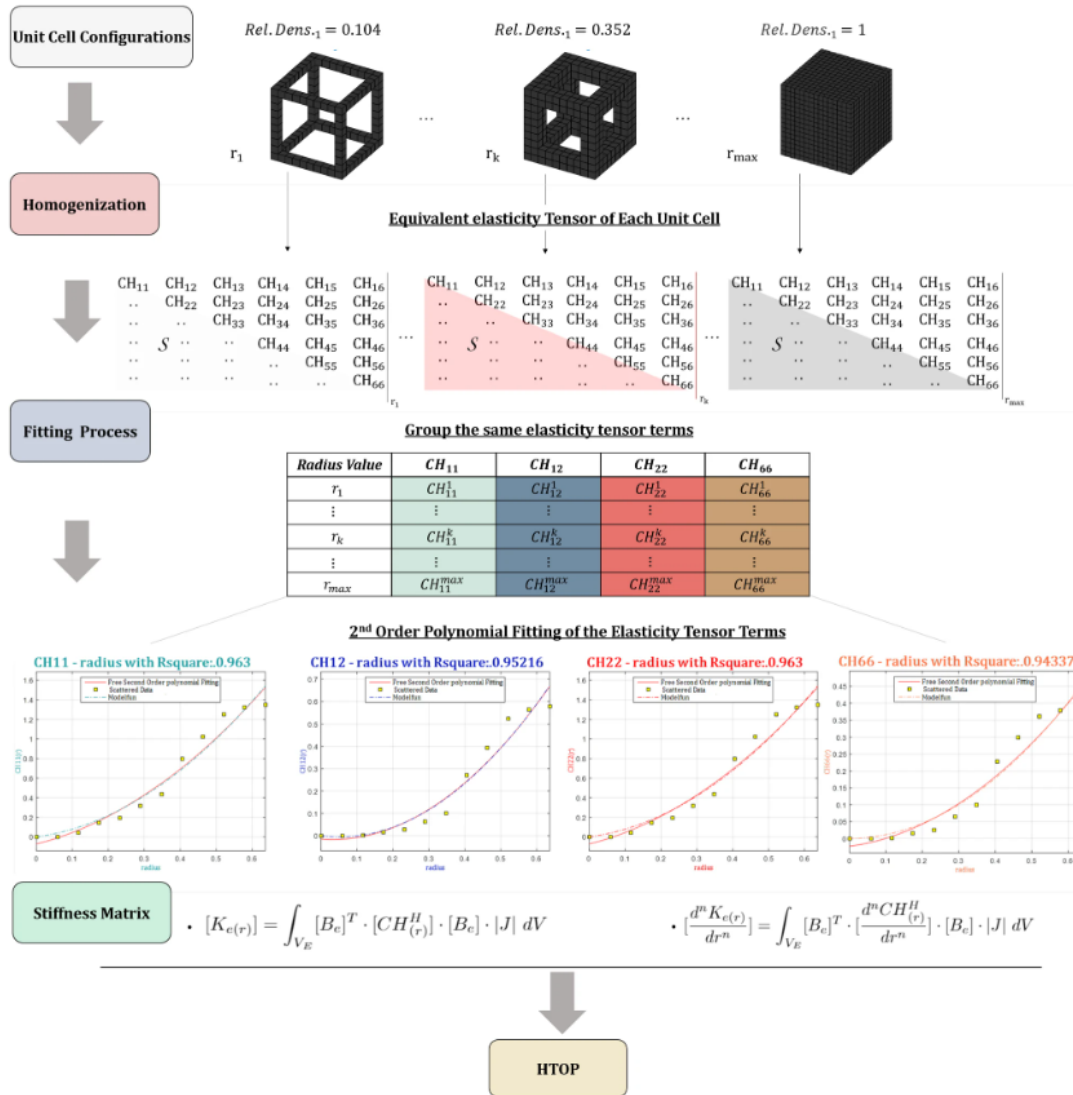


Figure 1.1: Homogenizing the unit cell, flowchart of the proposed methodology,[23]

### Section 1.3 Overview of Topology Optimization Under Uncertainty

In engineering practice, uncertainties are critical factors that must be considered, yet due to the complexity of stochastic calculations, designers often rely on deterministic data. To address this, stochastic programming and probabilistic notation have been introduced to the design process by incorporating probabilistic inequalities as constraints and acknowledging uncertainties in applied loading, which are best described using probabilistic methods [21, 3].

Historically, topology optimization literature that accounted for uncertainties was scarce until the late 20th century, although some exceptions considered multiple load or reliability constraints. Research has expanded to include uncertainties not only in loading conditions but also in support conditions and material properties, leading to three main groups of uncertainty handling in topology optimization: 1) structures built as designed with uncertain loads, 2) deterministic loads with uncertain nodal locations, and 3) robust optimization strategies using perturbation methods to handle uncertain material properties or geometry [4]. The field has seen significant growth over the past twelve years, with many studies aiming to reformulate uncertainties into an alternate deterministic formulation, often using statistical averages or higher order statistics to achieve robust design optimization.

Califore and Dabbene [11] have utilized two standard theorems to find optimal solutions of uncertain convex optimization problems in the context of truss topology optimization mainly on incorporating uncertainty in both the load pattern and material characteristics. The first approach involves minimizing the expected value of the objective function with respect to uncertainty, commonly known as the average approach. In the second approach, known as the worst-case or min-max approach, the objective is to minimize the worst-case objective. This approach involves considering the most unfavorable scenario by selecting the design that performs the best under the worst possible conditions. Both of these approaches have been proven to yield exact and computationally efficient solution schemes, particularly when the uncertainty can be modeled in a simplified manner.

The works of Lógó et al. [18, 17], Lógó [15, 16], and Pintér et al. [19] offer a suitable tool for conducting continuum type topology optimization procedures that account for uncertainty in applied loads. These publications employ a first-order approximation for compliance to address the presence of uncertainty.

### Section 1.4 Software Utilized in Our Research

In my research, the analysis and simulations will be conducted using MATLAB, a powerful and versatile computational platform. The methodology will involve leveraging a fast and advanced code previously established by Ferrari and Sigmund [13] as a foundational base. This code, detailed in their paper, "A new generation 99 line Matlab code for compliance topology optimization and its extension to 3D," will be thoroughly adapted and expanded upon to align with the specific requirements and objectives of our study.

## Chapter 2

# Topology Optimization for Loads with Multiple Points of Application

Most of the contributions dealing with multi-scale design are based on the volume-constrained minimum compliance problem, while a displacement-constrained minimum volume formulation is ideally conceived to investigate lightweight design at the serviceability limit state. Indeed, displacement limits are prescribed for structural elements by technical codes, whereas the amount of material needed to fulfil these constraints is an outcome of the design problem.

When it comes to multiple load cases, a classical extension of the minimum compliance problem consists in using a weighted sum of the energy contribution pertaining to each one of the considered load cases. However, when local control of the deflection is requested under the effect of distributed loads, multiple forces and multiple load cases, the enforcement of a set of displacement constraints is required.

When the controlled displacement is that at single loaded point along the direction of the applied force, the work of the external load at equilibrium equals the scalar product of the controlled displacement and the applied force. In this case, the displacement-constrained minimum volume problem is equivalent to a classical volume-constrained minimum compliance problem. As discussed in [1], the same solution (up to a scaling) is expected to arise when considering either problem. This rationale does not apply when multiple loading or distributed loads are dealt with.

### Section 2.1 Problem Statement

Standard four-node displacement-based membrane elements are used to get a discretization of a given design domain. A discrete design variable is assigned to each element. In the  $e$ -th of the  $n$  elements belonging to the mesh,  $0 \leq \rho_e \leq 1$  is the so-called "density" of the material. Using SIMP, the constitutive matrix  $\mathbf{C}(\rho_e)$  reads:

$$\mathbf{C}(\rho_e) = \rho_e^p \mathbf{C}_0 + \mathbf{C}_{min}, \quad (2.1)$$

where  $\mathbf{C}_0$  is the plane stress constitutive matrix at full density,  $\mathbf{C}_{min} = 10^{-9}\mathbf{C}_0$  stands for "void" and  $p$  is an interpolation parameter that penalizes intermediate densities, see in particular [13]. In the numerical simulations,  $p$  is increased from 3 to 9 during the optimization by means of the continuation approach used in the referenced work.

The statement of the displacement-constrained problem of minimum volume topology optimization, is:

$$\left\{ \begin{array}{l} \min_{0 \leq \rho_e \leq 1} V = \sum_{e=1}^n \rho_e V_{0,e} \quad (2.2a) \\ \text{subject to } \left( \sum_{e=1}^n \rho_e^p \mathbf{K}_{0,e} \right) \mathbf{U}_j = \mathbf{F}_j, \quad \text{for } j = 1 \dots l, \quad (2.2b) \\ \left\{ \begin{array}{l} u_i \cdot \text{sign}(u_{lim,i}) \leq |u_{lim,i}|, \\ \text{sign}(u_i) = \text{sign}(u_{lim,i}) \end{array} \right. \quad \text{for } i = 1 \dots m. \quad (2.2c) \end{array} \right.$$

In the above problem, the objective function shown in Eqn.(2.2a) is the volume of the structural element  $V$ . This may be computed through the sum over the contributions  $\rho_e V_{0,e}$ , being  $V_{0,e}$  the volume of the  $e$ -th element at full density, that is for  $\rho_e = 1$ .

Eqn.(2.2b) prescribes the static equilibrium of the structural element under multiple load cases. The global stiffness matrix is given by the element contributions accounting for the constitutive law of Eqn.(2.1). The element stiffness matrix reads  $\rho_e^p \mathbf{K}_{0,e}$ , where  $\mathbf{K}_{0,e}$  refers to  $\rho_e = 1$ . For the  $j$ -th of the  $l$  load cases,  $\mathbf{F}_j$  is the load vector, and  $\mathbf{U}_j$  is the relevant nodal displacement vector.

The  $i$ -th of the  $m$  displacement components to be controlled is denoted by  $u_i$ . Eqn.(2.2c) enforces a prescribed limit  $u_{lim,i}$ . This quantity  $u_{lim,i}$  stands for the maximum value that the  $i$ -th displacement component is allowed to undergo at the serviceability limit state. Assuming that  $u_i$  is an entry of  $\mathbf{U}_j$ , meaning that the  $i$ -th constraint refers to the  $j$ -th load case, one has:

$$u_i = \mathbf{L}_i^T \mathbf{U}_j, \quad (2.3)$$

where  $\mathbf{L}_i$  is a vector made of zeros with the exception of the entry referring to the  $i$ -th displacement degree of freedom, which takes unitary value.

## Section 2.2 Numerical Implementation

In this section, an insight is given on the treatment of the density field to avoid well-known numerical instabilities while achieving crisp black/white layouts, and on the gradient-based approach used to handle the arising multi-constrained problem.

A linear filter [8, 9] is implemented on the element variables  $\rho_e$  to avoid the arising of checkerboard patterns and mesh dependence.

The optimization problem in Eqn.(2.2) is solved via mathematical programming, using the Method of Moving Asymptotes (MMA) as minimizer. Displacement constraints are treated following the augmented Lagrangian method implemented in [14]. Constraints are

gathered in a modified version of the objective function such that the problem is turned into an unconstrained minimization. At the  $k$ -th AL step, this objective function reads:

$$V = V + \frac{1}{m} \sum_{i=1}^m \left( a_i^{(k)} \frac{|u_i|}{|u_{lim,i}|} + \frac{1}{2} b^{(k)} \left( \frac{u_i}{u_{lim,i}} \right)^2 \right), \quad (2.4)$$

where  $a_i^{(k)}$  is the  $i$ -th entry of the vector of the Lagrangian multiplier estimators and  $b^{(k)} > 0$  is a penalty factor.

The adjoint method is used to compute derivatives in order to provide the gradient-based minimizer with the sensitivity with respect to the design variables.

### Section 2.3 Results

A topology optimization formulation based on the distribution of isotropic material has been worked for identifying structures of minimal volume while adhering to multiple displacement constraints. This problem accommodates fixed points or distributed loads, incorporating loads with various points of application, in which a static moving force can be applied, with a local enforcement to control the relevant displacement.

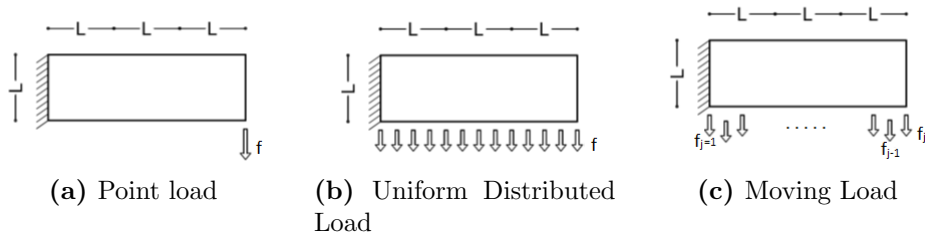


**Figure 2.1:** Cantilever beam: Initial problem

Numerical simulations have demonstrated optimal designs characterized by multiple displacement constraints. where two methodologies have been examined for the formulation of deflection enforcement: adhering to conventional practices at the serviceability limit state, wherein a uniform upper bound for displacement is applied across all controlled points, and employing a variable limit that mimic the stiffness exhibited by a full material beam.

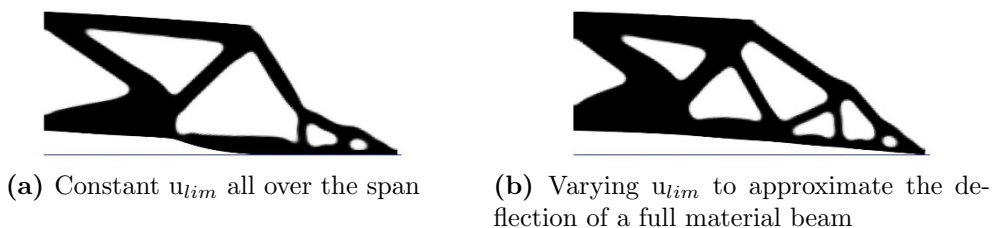


**Figure 2.2:** Cantilever beam: deformed shapes of the layouts achieved considering a uniformly distributed load

## Section 2.4 Conclusions

A topology optimization formulation using the distribution of isotropic material has been developed for structures of minimal volume that adhere to multiple displacement constraints and can accommodate fixed points or distributed loads, including a static moving force with local displacement control. A modified augmented Lagrangian approach with sequential convex programming efficiently handles the complexities of multi-constrained problems to achieve optimal designs. Numerical simulations have demonstrated optimal designs with multiple displacement constraints, where deflection enforcement strategies—either adhering to conventional practices at the serviceability limit state with a uniform upper bound or employing a variable limit that mimics full material beam stiffness—significantly impact the displacement observed under moving loads. Optimal solutions for moving loads compared to classical solutions for fixed loads show that the topology for moving loads is a slightly heavier variation of the topology for a single force applied at maximum deflection points.

## Chapter 3

# Lightweight Additive Design: Graded Porosity with Displacement Constraints

Porous structures exemplify the advanced features achievable via 3D printing, serving as a key model for the production of lightweight, robust, and multifunctional infills. These structures are often preferred over their solid counterparts for components with predetermined geometries. Among the techniques available for addressing the optimal design of infill and external shapes, multi-scale topology optimization presents an effective and efficient alternative within the same computational framework.

Building on these principles, the chapter introduces a multi-scale topology optimization approach for designing lightweight components that adhere to specified load and displacement limits. This method utilizes hexagonal close-packed arrangements of circular or spherical holes to define 2D or 3D isotropic or transversely isotropic microstructures, where the macroscopic elastic properties depend on the cavity radius, reflecting the material's density. An interpolation law is employed to manage multi-material structures, incorporating both solid and graded materials within a specified density range. This approach also indicates the position of the boundaries of the component and the potential internal configurations of holes facilitating the creation of optimal infill.

### Section 3.1 A Two-Phase Material Model with Void

Homogenization combines the properties of each discrete component that constitutes the composite material in order to extract its equivalent properties. By means of the homogenization theory the equivalent properties of an isolated from the composite's microstructure unit cell are obtained. The property of the composite material intended to be homogenized is the elasticity tensor of the non-homogeneous unit cell.

Andreassen [2] provided an efficient way to determine effective macroscopic properties, such as the elasticity tensor using a self-contained Matlab implementation which computes the effective elasticity tensor of a two material composite, where one material could be void. Andreassen [2] provided self-contained matlab code base on numerical homogenization method for 3D cellular materials that shows how the homogenized constitutive matrix is computed by a voxel model with one material to be void and another material

to be solid.

The material density of a two-dimensional graded porous microstructure featuring an hexagonal arrangement of circular holes can be computed as  $\rho_g = 1 - |Y_v|/|Y|$ , where  $|Y|$  is the volume of the base cell with dimensions  $l_{y1} = d, l_{y2} = \sqrt{3}d$  and  $|Y_v|$  is the volume of the inner circular-like voids.

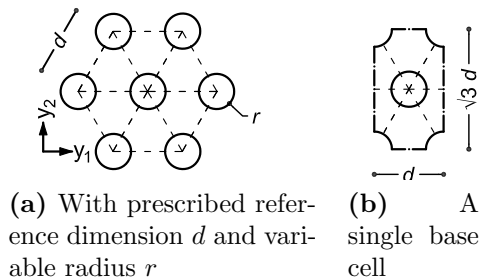


**Figure 3.1:** 2D version of the porous microstructure hexagonal arrangement of circular holes

The density depends upon the radius of the circular holes as:

$$\rho_g = 1 - \frac{2\pi r^2}{\sqrt{3}d^2} \quad \text{for } 0 \leq r \leq r_{max}, \quad \text{with } r_{max} = \frac{d-t}{2}, \quad (3.1)$$

where  $r_{max}$  is the maximum radius as a function of the reference dimension of the microstructure,  $d$ , and of the minimum thickness of the material between two adjacent holes,  $t$ .

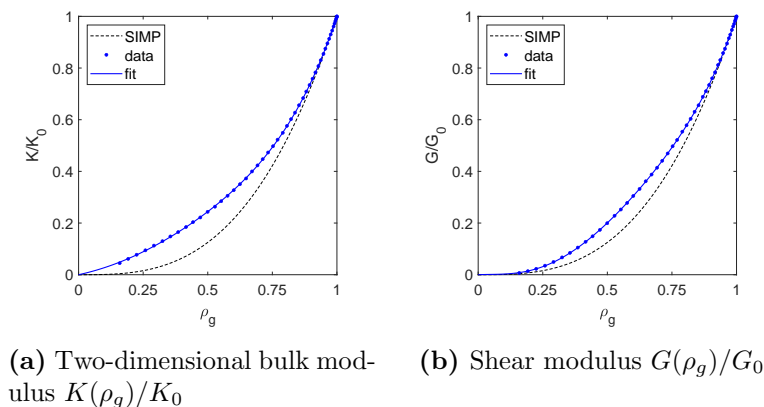


**Figure 3.2:** 2D version of the porous microstructure: interpolation laws fitting results from numerical homogenization, as compared to the conventional SIMP

For transversally isotropic material the stress-strain relationship is a function of five independent parameters. Its dependence on  $\rho_g$  can be evaluated by applying the voxel-based homogenization approach presented in [12] to the base cell of Figure 3.3.

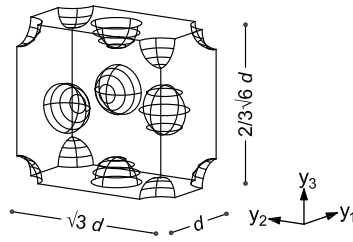


**Figure 3.3:** 3D version of the porous microstructure: three dimensional view of a single base cell

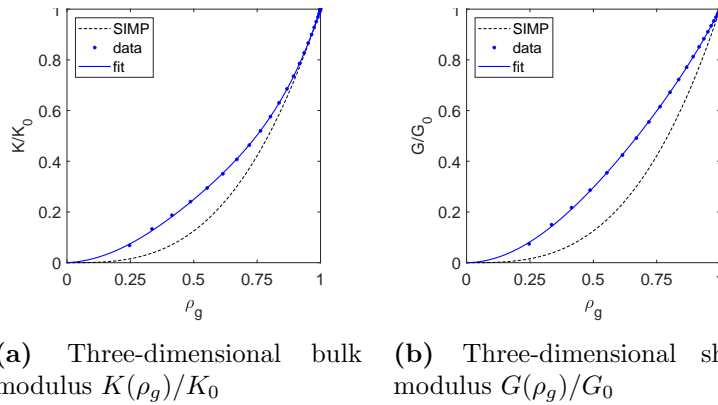


**Figure 3.4:** 3D version of the porous microstructure: interpolation laws fitting results from numerical homogenization, as compared to the conventional SIMP

A two-phase interpolation law for the isotropic elastic constants is introduced to allow for the distribution of full material and void, along with a fraction of porous microstructure with graded circular/spherical holes. It reads:

$$\begin{aligned} K(\rho, \rho_g) &= \rho^p K_0 + (1 - \rho^p) K(\rho_g), \\ G(\rho, \rho_g) &= \rho^p G_0 + (1 - \rho^p) G(\rho_g), \end{aligned} \quad (3.2)$$

for  $0 \leq \rho, \rho_g \leq 1$ .

For  $\rho = 1$ , whatever the value of  $\rho_g$ , the bulk modulus and the shear one are those of full material, i.e.  $K_0$  and  $G_0$  respectively. For  $\rho = \rho_g = 0$ , only the terms  $K_{min}$  and  $G_{min}$  are nonzero, i.e. the fictitious stiffness of the void is found. For  $\rho = 0$  and  $\rho_g \neq 0$  a porous microstructure may arise according to the adopted interpolation.

In the above equations, the penalization of  $\rho$  is especially conceived to steer the design towards its limit values, i.e.  $\rho = 1$  (full material) or  $\rho = 0$  (void or porous microstructure graded by  $\rho_g$ ). Indeed, increasing  $\rho$  on a certain place automatically reduces the weight of the complementary phase, thus promoting 0-1 design.

## Section 3.2 Formulation

A finite element discretization of a given design domain is operated, using four-node and eight-node displacement-based elements in two and three dimensions, respectively.

Two sets of element-wise design variables are considered to implement the material law of Eqn.(3.2). In the  $e$ -th of the  $n$  elements of the mesh,  $\rho_e$  and  $\rho_{g,e}$  are the discrete counterpart of the variables  $\rho$  and  $\rho_g$ , respectively.

A problem for the design of a topology of minimum weight under displacement constraints can be stated as:

$$\left\{ \begin{array}{l} \min_{\substack{0 \leq \rho_e \leq 1 \\ 0 \leq \rho_{g,e} \leq \rho_{g,max}}} V = \sum_{e=1}^n \left( \rho_e + (1 - \rho_e) \rho_{g,e} \right) V_{0,e} \quad (3.3a) \\ \text{s.t. } \mathbf{K}(\boldsymbol{\rho}, \boldsymbol{\rho}_g) \mathbf{U}_j = \mathbf{F}_j, \quad \text{for } j = 1 \dots l, \quad (3.3b) \\ \left\{ \begin{array}{l} u_i \cdot \text{sign}(u_{lim,i}) \leq |u_{lim,i}|, \quad \text{for } i = 1 \dots m \\ \text{sign}(u_i) = \text{sign}(u_{lim,i}) \end{array} \right. \quad (3.3c) \\ \sum_{e=1}^n (1 - \rho_e) \rho_{g,e} V_{0,e} \geq f_g \sum_{e=1}^n V_{0,e}. \quad (3.3d) \end{array} \right.$$

In the above statement, the objective function is the weight of the component, which is computed through the sum of the element contributions  $(\rho_e + (1 - \rho_e) \rho_{g,e}) V_{0,e}$ , being  $V_{0,e}$  the volume of the  $e$ -th element for  $\rho_e = 1$ .

Eqn.(3.3b) prescribes the discrete elastic equilibrium. The global stiffness matrix  $\mathbf{K}(\boldsymbol{\rho}, \boldsymbol{\rho}_g)$  is computed by assembling the element contributions that account for the constitutive law given in Eqn.(3.2). Each of them may be conveniently written as the sum of a contribution depending on the interpolation of the bulk modulus  $K(\rho_e, \rho_{g,e}) \mathbf{K}_{K0,e}$ , and a contribution depending on the shear modulus  $G(\rho_e, \rho_{g,e}) \mathbf{K}_{G0,e}$ , where  $\mathbf{K}_{K0,e}$  and  $\mathbf{K}_{G0,e}$  both refer to  $\rho_e = 1$ , see also [10]. For the  $j$ -th of the  $l$  load cases,  $\mathbf{F}_j$  is the load vector, whereas  $\mathbf{U}_j$  is the corresponding nodal displacement vector.

Eqn.(3.3d) prescribes a minimum value for the weight fraction of the porous microstructure, namely  $f_g$ .

### Section 3.3 Post-Processing for Manufacturing

As a result of the minimization procedure, an optimal distribution of the element unknowns  $\rho_e$  and  $\rho_{g,e}$  is found throughout the design domain. The boundaries of the object are detected by processing the distribution of the overall material density, namely  $\rho_e + (1 - \rho_e) \rho_{g,e}$ , thus handling together both the solid material region, i.e.  $\rho_e$ , and the graded material one, i.e.  $(1 - \rho_e) \rho_{g,e}$ .

For the generic hole, the average value of the quantity  $(1 - \rho_e) \rho_{g,e}$  is computed over the elements falling within a neighbourhood of its center with diameter  $d/2$ , and denoted by  $\bar{\rho}_g$ . No hole is allowed if any of the surrounding elements falling within the area defined above has  $\rho_{g,e} = 0$  or  $\rho_e = 1$ . In 2D, according to Eqn.(3.1), the radius of a circular hole reads:

$$r = \left( \frac{(1 - \bar{\rho}_g)\sqrt{3}}{2\pi} \right)^{1/2} d. \quad (3.4)$$

The final geometry is given by Boolean subtraction of the simple geometrical entities representing the holes (circles or spheres) from the shape representing the region within the external boundaries.

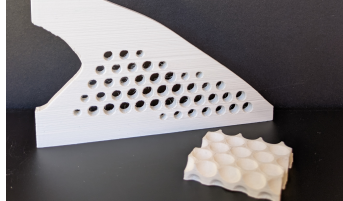


**Figure 3.5:** Test specimens fabricated by means of Fused Deposition Modeling without the need of supports.

### Section 3.4 Results

Numerical examples are presented to assess the method introduced earlier, considering two- and three- dimensional applications. The constraints enforced to govern the deflection are such that, in each one of the considered nodes, the controlled component of the displacement cannot overcome  $\alpha$  times that computed adopting  $\rho = 1$  everywhere (full material in the entire design domain). In the two- dimensional numerical applications it is assumed that  $\alpha = 1.5$ , whereas  $\alpha = 2.5$  is used for the three-dimensional example.

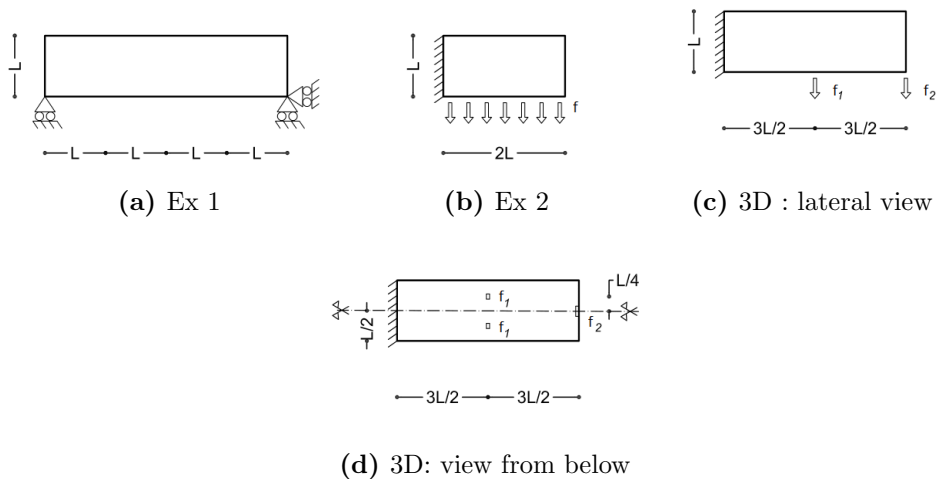
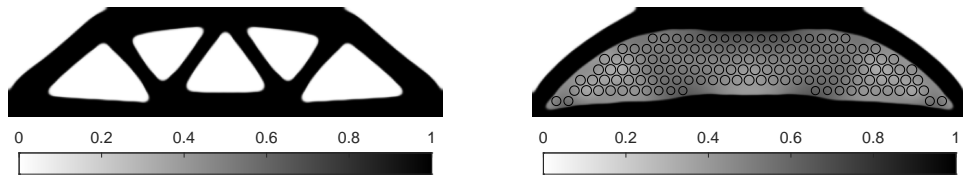
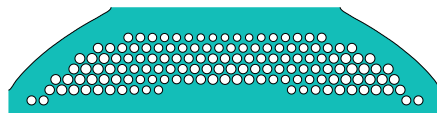


**Figure 3.6:** Geometry and boundary conditions for the two-dimensional numerical examples.

The approach yields coated structures, where a solid coating encloses a region of porous material, adaptable to various load types and displacement constraints. The optimization procedure intrinsically determines the thickness and location of these coatings. Furthermore, full-scale finite element analyses conducted on two-dimensional blueprints, consid-



(a) Example 1. Optimal design for  $f_g = 0$ ,  $V/V_0 = 0.533$ . (b) Overlay of the HPC circular holes and of the optimal distribution of material density



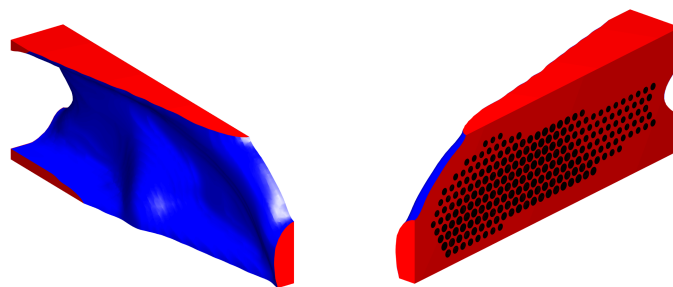
(c) Final layout

**Figure 3.7:** Example 1. Design for  $f_g = 0.20$ ,  $d=L/9$  (a); final layout (b).

ering varying sizes of the porous microstructure, have validated the approach, showing a good correlation between computed and predicted displacements.

|       | Load type         | Multi-scale design |         |           | Full-scale analysis of blueprints |         |           |
|-------|-------------------|--------------------|---------|-----------|-----------------------------------|---------|-----------|
|       |                   | Layout             | $V/V_0$ | $v^{max}$ | Layout                            | $V/V_0$ | $v^{max}$ |
| Ex. 1 | $f_1 = f_2 = f_3$ | 0-1                | 0.533   | 7.44      | truss                             | 0.555   | 7.18      |
|       |                   | Graded             | 0.596   | 7.58      | Final Layout ( $d = L/9$ )        | 0.628   | 6.82      |
| Ex. 2 | $f$               | 0-1                | 0.556   | 4.56      | truss                             | 0.569   | 4.36      |
|       |                   | Graded             | 0.578   | 4.56      | Final Layout; ( $d = L/12$ )      | 0.608   | 4.21      |
|       | $f_{var}$         |                    |         |           | Final Layout ( $d = L/16$ )       | 0.598   | 4.26      |
|       |                   |                    |         |           | truss                             | 0.569   | 4.99      |
|       |                   |                    |         |           | Final Layout ( $d = L/12$ )       | 0.608   | 4.53      |
|       |                   |                    |         |           | Final Layout ( $d = L/16$ )       | 0.598   | 4.61      |

**Table 3.1:** Multi-scale design vs. full-scale finite element analysis of the blueprints: values of the maximum deflection under the loaded points  $v^{max}$  (mm).



(a) External view (b) Internal view

**Figure 3.8:** 3D Final design for:  $f_g = 0.10$ ,  $V/V_0 = 0.274$ ,  $d = L/12$

### Section 3.5 Conclusions

A multi-scale topology optimization approach is developed for designing structural components to achieve minimum weight with specific load and displacement constraints. The method uses numerical homogenization to characterize the macroscopic elastic properties of hexagonal close-packed structures with circular and spherical cavities, considering the cavities' radii. It applies an isotropic constitutive law in two-dimensional scenarios and a transversely isotropic law for three-dimensional microstructures to handle moderate anisotropy, deriving properties in terms of bulk and shear moduli across varying densities. The research introduces a multi-material interpolation law for distributing solid, graded porous phases, and void, enhanced by filtering and projection techniques to ensure smooth density distributions and appropriate material placement. The optimization yields structures with distinct material phases and a solid coating around porous regions, adjusted for various loads and displacements. Finite element analyses confirm the method's effectiveness, with preliminary tests on additive manufacturing showing potential for creating extended cavities with graded materials.

## Chapter 4

# Topology Optimization with Graded Infill for Loading Uncertainty

In this chapter, the design optimization of composite structures comprising a solid phase and a specified fraction of graded infill is addressed. Utilizing homogenization-based topology optimization, the analysis incorporates uncertainties in loading amplitude. A two-phase material law incorporating void space is implemented to regulate both the distribution and permissible density of the graded infill. Numerical homogenization techniques are employed to ascertain the macroscopic elastic properties of isotropic and two types of orthotropic infills, prevalent in additive manufacturing applications.

The formulation of a minimum weight problem is enhanced by deterministic displacement constraints, which equivalently address probabilistic displacement enforcements under the assumption of normally distributed force amplitudes. The multi-constrained optimization problem is approached through sequential convex programming, facilitating an efficient resolution method in line with the approaches devised in the previous chapters.

### Section 4.1 Material Law

A two-phase interpolation law is adopted to distribute full material and void, along with a fraction of a porous graded microstructure with prescribed layout. Assuming plane stress conditions, the constitutive law for the herein considered linear elastic material reads  $\underline{\sigma} = \mathbf{C}\underline{\varepsilon}$ , where:

$$\mathbf{C}(\rho_1, \rho_2, \rho_g) = \mathbf{C}_{min} + \rho_1^p(\mathbf{C}_0 - \mathbf{C}_{min}) + \rho_2^p(1 - \rho_1^p)(\mathbf{C}_H(\rho_g) - \mathbf{C}_{min}), \quad (4.1)$$

with penalization  $p \geq 3$ . In the above equation,  $0 \leq \rho_1, \rho_2 \leq 1$  and  $\rho_{g,min} \leq \rho_g \leq \rho_{g,max}$  are three variables governing the material law, being  $\rho_{g,min}$  and  $\rho_{g,max}$  the bounds of the admissible density range of the porous phase. For  $\rho_1 = 1$ , whatever the value of  $\rho_2$  and  $\rho_g$ , the constitutive matrix is that of full material, i.e.  $\mathbf{C}_0$ . For  $\rho_1 = \rho_2 = 0$ , independently on the value of  $\rho_g$ , only the terms  $\mathbf{C}_{min}$  survives, meaning that a fictitious stiffness that stands for void is found. For  $\rho_1 = 0$  and  $\rho_2 = 1$ , a porous microstructure may arise with a macroscopic stiffness tensor  $\mathbf{C}_H$  that depends on the density of the porous phase  $\rho_g$ ,

according to the following interpolation:

$$\mathbf{C}_H = \begin{bmatrix} c_{H,11}(\rho_g)C_{0,11} & c_{H,12}(\rho_g)C_{0,12} & 0 \\ & c_{H,22}(\rho_g)C_{0,22} & 0 \\ \text{sym} & & c_{H,33}(\rho_g)C_{0,33} \end{bmatrix}. \quad (4.2)$$

The dependence of the macroscopic stress-strain matrix  $\mathbf{C}_H$  on the density of the porous phase  $\rho_g$  is evaluated by performing numerical homogenization on the base cells represented in Figure 4.1

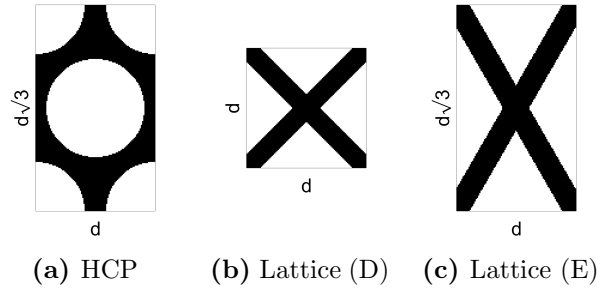


**Figure 4.1:** Base cells used in the numerical studies (for  $\rho_g = 0.40$ )

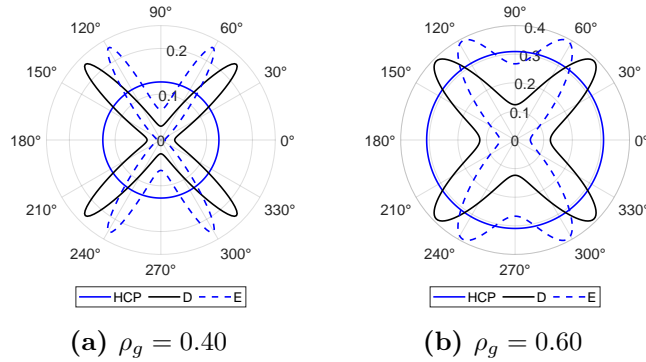


**Figure 4.2:** Apparent Young's modulus of the hexagonal close-packing of circular holes (HCP), diamond lattice (D) and elongated diamond lattice (E), depending on the orientation of the reference system. Values are scaled with respect to that of the full isotropic material phase.

## Section 4.2 Probabilistic Formulation

A finite element discretization of a given design domain is operated, using four-node displacement-based plane stress elements. Three sets of element-wise design variables are considered to implement the linear elastic material law of Eqn.(4.1). In the  $e$ -th of the  $n_e$  elements of the mesh,  $\rho_{1,e}$ ,  $\rho_{2,e}$  and  $\rho_{g,e}$  are the discrete counterpart of the unknown fields  $\rho_1$ ,  $\rho_2$  and  $\rho_g$ , respectively.

A set of  $l$  probabilistic point loads acting simultaneously is considered. The intensity of the  $j$ -th force  $f_j$  is a random variable with normal (Gaussian) distribution and mean value  $\bar{f}_j$ . The covariance matrix is denoted as  $\mathbf{K}_{ov}$ , whose components are  $k_{a,b}$ .

A problem for the design of a topology of minimum weight under displacement constraints can be stated as:

$$\left\{ \begin{array}{l} \min_{\substack{0 \leq \rho_{1,e}, \rho_{2,e} \leq 1 \\ \rho_{g,min} \leq \rho_{g,e} \leq \rho_{g,max}}} V = \sum_{e=1}^n \left( \rho_{1,e} + (1 - \rho_{1,e}) \rho_{2,e} \rho_{g,e} \right) V_{0,e} \quad (4.3a) \\ \text{s.t. } \mathbf{K}(\boldsymbol{\rho}_1, \boldsymbol{\rho}_2, \boldsymbol{\rho}_g) \mathbf{U}_j^{unit} = \mathbf{F}_j^{unit}, \quad \text{for } j = 1 \dots l, \quad (4.3b) \\ P(u_i \leq u_{lim,i}) \geq 1 - P_{fail}, \quad \text{for } i = 1 \dots m, \quad (4.3c) \\ \sum_{e=1}^n (1 - \rho_{1,e}) \rho_{2,e} \rho_{g,e} V_{0,e} \geq f_g \sum_{e=1}^n V_{0,e}. \quad (4.3d) \end{array} \right.$$

In the above statement, the objective function is the weight of the component, which is computed through the sum of the element contributions  $(\rho_{1,e} + (1 - \rho_{1,e}) \rho_{2,e} \rho_{g,e}) V_{0,e}$ , being  $V_{0,e}$  the volume of the  $e$ -th element for  $\rho_e = 1$ . In this sum, the first term addresses full material, whereas the second the graded one.

Eqn.(4.3b) prescribes the discrete elastic equilibrium. For the  $j$ -th of the  $l$  forces acting simultaneously on the domain,  $\mathbf{F}_j^{unit}$  is the load vector that refers to a unit force with same point of application and direction of  $f_j$ , and  $\mathbf{U}_j^{unit}$  is the corresponding nodal displacement vector.

The  $i$ -th of the  $m$  displacement components to be controlled is denoted by  $u_i$ . Eqn.(4.3c) enforces the probability that  $u_i$  does not exceed  $u_{lim,i}$  to be at least equal to a prescribed value  $1 - P_{fail}$ , being  $u_{lim,i}$  for the relevant maximum displacement allowed and  $P_{fail}$  the accepted failure probability.

According to [20], if  $\xi_1, \xi_2, \dots, \xi_s$  have a joint normal distribution, then the vector  $\mathbf{x} \in \mathbb{R}^s$  with components  $x_1, x_2, \dots, x_s$  satisfying:

$$P \left( \sum_{h=1}^s x_h \xi_h \leq 0 \right) \geq q, \quad (4.4)$$

is the same as that satisfying:

$$\sum_{h=1}^s x_h \bar{\xi}_h + \Phi^{-1}(q) \left( \mathbf{x}^T \mathbf{K}_{ov} \mathbf{x} \right)^{1/2} \leq 0, \quad (4.5)$$

where  $\bar{\xi}_h$  is the mean value of  $\xi_h$ ,  $\mathbf{K}_{ov}$  is the covariance matrix of the random vector  $\boldsymbol{\xi}$ , and  $\Phi^{-1}(q)$  is the inverse cumulative distribution function of the normal distribution (probit function), evaluated at the prescribed probability  $f$ .

The probabilistic constraint of Eqn.(4.3c) may be re-written in the form:

$$P \left( \sum_{j=1}^l u_{i,j}^{unit} f_j - u_{lim,i} \leq 0 \right) \geq 1 - P_{fail}. \quad (4.6)$$

According to Eqns.(4.4-4.5), since it has been assumed that  $f_1, f_2, \dots, f_l$  have a joint nor-

mal distribution, then the vector  $\mathbf{u}_i^{unit}$  with components  $u_{i,1}^{unit}, u_{i,2}^{unit}, \dots, u_{i,l}^{unit}$  satisfying Eqn.(4.6) is the same as that satisfying:

$$\sum_{j=1}^l u_{i,j}^{unit} \bar{f}_j + \Phi^{-1}(1 - P_{fail}) \left( (\mathbf{u}_i^{unit})^T \mathbf{K}_{ov} \mathbf{u}_i^{unit} \right)^{1/2} - u_{lim,i} \leq 0, \quad (4.7)$$

where  $-u_{lim,i}$  of Eqn.(4.6) may be straightforwardly handled through Eqns.(4.4-4.5) by introducing the slack variables  $x_{s+1} = -1$  and  $\xi_{s+1} = u_{lim,i}$ , the latter with zero variance and zero covariance, see [15].

The above deterministic inequality will be implemented in Eqn.(4.3), instead of the original probability constraint.

Eqn.(4.3d) prescribes a minimum value for the weight fraction of the porous microstructure, namely  $f_g$ . A lower bound  $\rho_{g,min}$  applies due to manufacturing constraints. An upper bound  $\rho_{g,max}$  is prescribed, as well. Both bounds are enforced in Eqn.(4.3) through the statement of side constraints for the variables  $\rho_{g,e}$ .

### Section 4.3 Results

A numerical examples is presented to assess the method. The constraints enforced to govern the deflection are such that, in each one of the considered nodes, the controlled component of the displacement is not allowed to exceed  $\alpha$  times that computed adopting  $\rho_1 = 1$  everywhere,  $\alpha = 2.5$  is used in this example. Geometry and boundary conditions are those presented in Figure 4.3. The filter radii used in the simulations are  $r_{1,f} = r_{2,f} = L/10$ , for  $\rho_{1,e}$  and  $\rho_{2,e}$ , whereas  $r_{g,f} = 3 \times L/10$  is adopted for  $\rho_{g,e}$ . Solutions are generated by enforcing different values of  $f_g \geq 0$  in the formulation of Eqn.(4.3). In the example below,  $L = 100$  unit length, and mean value of  $f = 1$  unit force, and  $P_{fail} = 0.1$  will be used throughout the numerical section.

The example addresses the simply-supported beam with overhangs represented. Four point forces are symmetrically applied at the lower edge of the rectangular design domain. The optimal design found for  $f_g = 0$  when considering the amplitude of the forces as deterministic and equal in value is represented in Figure 4.4. Two independent structures arise around the supports, whose rotational equilibrium requires  $f_1 = f_2$  and  $f_3 = f_4$ . No porous phase is found.

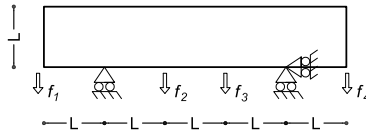


**Figure 4.3:** Geometry and boundary conditions

Assuming that the forces are uncorrelated, all with the same average value and coefficient of variation equal to 0.25, a completely constrained statically determinate structure arises,

see Figure 4.5. The weight at convergence of this 0-1 solution is  $V/V_0 = 0.497$ , with an increase not far from 60% with respect to the layout found in case of deterministic loads.



**Figure 4.4:** Optimal design in case of deterministic forces,  $V/V_0 = 0.315$ .



**Figure 4.5:** Optimal design in case of uncorrelated forces ( $CV = 0.25$  for all forces,  $P_{fail} = 0.1$ ),  $V/V_0 = 0.497$ .

Further numerical investigations are performed, focusing on uncorrelated forces and enforcing a minimum weight of the porous phase where  $f_g = 0.25$ . To avoid the arising of any unsupported region, one may leverage on the material law in Eqn.(4.1) by specifying "passive" domains for the variable  $\rho_{2,e}$ , see e.g. [5]. Indeed, by setting  $\rho_{2,e} = 1$  in a certain domain, either a solid phase or an infill region may arise there.



(a) HCP,  $V/V_0 = 0.563$



(b) Diamond lattice (D),  $V/V_0 = 0.530$



(c) Elongated diamond lattice (E),  
 $V/V_0 = 0.549$

**Figure 4.6:** Optimal design in case of uncorrelated forces ( $CV = 0.25$  for all forces,  $P_{fail} = 0.1$ ) enforcing  $f_g = 0.25$  and  $0.25 \leq \rho_g \leq 0.45$ , using passive regions for  $\rho_{2,e}$  and an infill.

The optimal layouts represented in Figure 4.5 and Figure 4.6 are further investigated addressing their structural response in case of correlated loads. In Table 4.1, maximum values of the probability of failure for the considered displacement constraints are reported, addressing the four different cases.

$$\text{case } A: \quad r_{12} = r_{23} = r_{34} = 0.5, \quad r_{13} = r_{24} = -0.5, \quad r_{14} = -1,$$

$$\text{case } B: \quad r_{12} = r_{13} = r_{14} = r_{23} = r_{24} = r_{31} = -0.33,$$

$$\text{case } C: \quad r_{12} = r_{13} = r_{24} = r_{34} = -1, \quad r_{14} = r_{23} = 1,$$

$$\text{case } D: \quad r_{12} = r_{14} = r_{23} = r_{34} = -1, \quad r_{13} = r_{24} = 1.$$

The 0-1 layout achieved in case of uncorrelated forces exceeds the reference value (0.1) by a noticeable amount in the cases *B*, *C*, and *D*. For composite beams this happens only

in the cases  $B$  and  $C$ , thus confirming the effective structural contribution provided by the graded porous phase when dealing with the shear-dominated case  $D$ .

|                            | case $A$ | case $B$ | case $C$ | case $D$ |
|----------------------------|----------|----------|----------|----------|
| 0-1 design, Fig.4.5        | 0.078    | 0.128    | 0.214    | 0.140    |
| HCP-based design, Fig.4.6a | 0.100    | 0.125    | 0.240    | 0.101    |
| D-based design, Fig.4.6b   | 0.107    | 0.126    | 0.247    | 0.079    |
| E-based design, Fig.4.6c   | 0.108    | 0.125    | 0.245    | 0.087    |

**Table 4.1:**  $P_{fail}$  computed for the optimal layouts represented in Figure 4.5 and Figure 4.6, considering different cases of correlation of the forces.

## Section 4.4 Conclusions

A homogenization-based topology optimization method has been developed to design minimum weight structures considering uncertain load amplitudes, using a joint normal distribution function to address stochastic displacement constraints as deterministic enforcements. The method employs a two-phase material law incorporating voids to model composite structures with a solid phase and a specific fraction of graded infill.

Macroscopic elastic constants for isotropic and two orthotropic infills commonly used in additive manufacturing were derived through numerical homogenization. These include a hexagonal arrangement of circular holes and two diamond lattices designed for high stiffness-to-weight ratios and self-supporting structures. The optimization includes side constraints to control the porous phase density and ensure the distribution of graded infill. Simulations evaluated the method, revealing that uncertainties in loading lead to completely constrained designs, replacing layouts that are only partially constrained under deterministic forces. Notably, designs with a prescribed infill fraction and low values of  $\rho_{g,max}$ , resulted in coated structures with slightly increased overall weight, confirming their effectiveness in multi-load scenarios. Additionally, sandwich structures with self-supporting infill are shown to be suitable for layer-by-layer additive manufacturing, addressing overhang challenges. The simulations also highlighted that the specific lattice type significantly influences both the topology and structural performance under load uncertainties.

## Chapter 5

# New Scientific Results

### Section 5.1 Theses 1

I developed a topology optimization formulation that minimizes the volume of structures subjected to multiple displacement constraints. This formulation incorporates two deflection enforcement strategies: a uniform upper bound, typical of serviceability limit states, and a variable limit that match the stiffness characteristics of a fully materialized beam.

I utilized a modified augmented Lagrangian method integrated with sequential convex programming to address the complexity of multi-constraint optimization, ensuring efficient design solutions. The formulation accommodates both fixed and distributed loads, adaptable to varying application points of static moving forces.

Related publication: [III] [i]

### Section 5.2 Theses 2

- a) I developed a multi-scale topology optimization method for lightweight structural design, utilizing numerical homogenization to assess the properties of porous materials and implementing a mixed-material approach for optimal density distribution that utilizes hexagonal close-packed arrangements of circular or spherical holes to define 2D or 3D isotropic or transversely isotropic microstructures.
- b) I verified the method by achieving an optimal distribution of material density, enabling clear identification of solid and graded regions, and discussed post-processing techniques for defining component boundaries and internal structures. The approach also allows for the creation of coated structures adaptable to various loads and displacement constraints.

Related publication: [II] [ii] [b] [c]

### Section 5.3 Theses 3

- a) I proposed a numerical method of homogenization-based topology optimization, accounting for uncertainty in loading amplitude. By assuming a joint normal distribution for uncertainty and transforming probabilistic displacement constraints into deterministic enforcements, enabling the design of minimum weight structures with specific probabilities of exceeding displacement limits.
- b) I derived the macroscopic elastic constants of isotropic and orthotropic infills commonly used in additive manufacturing through numerical homogenization, and I adopted a two-phase material law with void to design composite structures composed of a solid phase and a fraction of graded infill with a prescribed layout. And I proved that partially constrained layouts typically seen in deterministic forces can be replaced by completely constrained ones under uncertainty. I also found that the type of graded lattice significantly affects the topology and structural performance under load uncertainties, indicating that the shape and locations of solid features and infill in coated structures are unique to the adopted porous microstructure.

Related publication: [IV] [iii] [a] [d]

### Section 5.4 List of Publications

#### 1. Journal Papers:

- I Lógó, János, and Ismail, Hussein. "Milestones in the 150 Years History of Topology Optimization: A Review." *Computer Assisted Methods in Engineering and Science* 27, 2–3 (2020): 97–132.
- II Bruggi, Matteo, Ismail, Hussein, Lógó, János, and Paoletti, Ingrid. "Lightweight Design With Displacement Constraints Using Graded Porous Microstructures." *Computers and Structures* 272 (2022): 106873.
- III Ismail, Hussein, Bruggi, Matteo, and Lógó, János. "Topology Optimization for Loads with Multiple Points of Application". *Acta Polytechnica Hungarica* 20, 1 (2023): 29–44.
- IV Bruggi, Matteo, Ismail, Hussein, and Lógó, János. "Topology Optimization with Graded Infill Accounting for Loading Uncertainty". *Composite Structures* 311 (2023): 116807.

#### 2. Conference Papers:

- i Bruggi M., Ismail H., Lógó, J., Optimal design with multiple displacement constraints, 12th IEEE International Conference on Cognitive Infocommunications – CogInfoCom 2021, September 23-25, 2021 (online) Proceedings with ISBN 978-1-6654-2495-0.

- ii Ismail H., Bruggi M., Lógó, J., Multiscale Optimal Design of Grid Systems for High-rise Buildings, WEO 2021 - 2nd Workshop on Engineering Optimization, 7-8 October 2021, Warsaw, Poland (online) Proceedings with ISBN 978-83-65550-23-1.
- iii Bruggi M., Ismail H., Lógó, J., An application of multiscale topology optimization with loading uncertainty, The Fourteenth International Conference on Computational Structural Technology 23-25 August 2022, Montpellier, France, Proceedings with ISSN 2753-3239.

### 3. Conference Abstracts:

- a J. Lógó, P. Tazowski, B. Błachowski, and H. Ismail. "Reliability-based approaches for topology optimization of elasto-plastic structures." In 25th International Congress of Theoretical and Applied Mechanics: Book of Abstracts, 2911-2912. Milan, Italy (2021). Paper: O106110-FS10.
- b Ismail H., Lógó, J., Bruggi M., Optimal design of grid systems for tall buildings using lattice structures In: Book of abstracts of the 14th World Congress of Structural and Multidisciplinary Optimization (WCSMO-14), Colorado, US (2021) p. 44. Paper: Abstract ID: 62.
- c Ismail H., Bruggi M., Lógó, J., "Integrating Porous Material in Light Weight Topology Optimization Designs." In Proceedings of Extended Abstracts 20th International Conference of Modelling in Mechanics, Technical University of Ostrava, Czech Republic (2022).
- d Bruggi M., Ismail H., Lógó, J., Multi-scale topology optimization of composite beams accounting for loading uncertainty. 25th International Conference on Composite of Structures, Porto, Portugal (2022).
- e Bruggi M., Ismail H., Lógó, J., Optimal design of reticulated shells accounting for strength, local buckling and overhang angles. 15th World Congress of Structural and Multidisciplinary Optimisation, Cork, Ireland (2023).

# Bibliography

- [1] W. Aichtziger. “Topology Optimization of Discrete Structures”. In: *Topology Optimization in Structural Mechanics*. Vienna, 1997, pp. 57–100.
- [2] E. Andreassen and Casper Schousboe Andreasen. “How to determine composite material properties using numerical homogenization”. In: *Computational Materials Science* 83 (2014), pp. 488–495.
- [3] André Teófilo Beck and Wellison José de Santana Gomes. “A comparison of deterministic, reliability-based and risk-based structural optimization under uncertainty”. In: *Probabilistic Engineering Mechanics* 28 (2012), pp. 18–29.
- [4] A Ben-Tal and A Nemirovski. “Robust convex optimization”. In: *Math. Oper. Res.* 23.4 (Nov. 1998), pp. 769–805.
- [5] Martin Philip Bendsoe and Ole Sigmund. *Topology optimization: theory, methods, and applications*. 2003.
- [6] L Berke. “An efficient approach to the minimum weight design of deflection limited structures”. In: *Rep. Air Force Flight Dynamics Lab* (1970).
- [7] L Berke and NS Khot. *Use of optimality criteria methods for large scale systems*. Air Force Flight Dynamics Laboratory, 1974.
- [8] Thomas Borrvall and Joakim Petersson. “Topology optimization using regularized intermediate density control”. In: *Computer Methods in Applied Mechanics and Engineering* 190.37 (2001), pp. 4911–4928.
- [9] Blaise Bourdin. “Filters in topology optimization”. In: *International Journal for Numerical Methods in Engineering* 50.9 (2001), pp. 2143–2158.
- [10] Matteo Bruggi. “Topology optimization with mixed finite elements on regular grids”. In: *Computer Methods in Applied Mechanics and Engineering* 305 (2016), pp. 133–153.
- [11] Giuseppe C Calafiore and Fabrizio Dabbene. “Optimization under uncertainty with applications to design of truss structures”. In: *Struct. Multidiscipl. Optim.* 35.3 (Mar. 2008), pp. 189–200.
- [12] Guoying Dong, Yunlong Tang, and Yaoyao Fiona Zhao. “A 149 Line Homogenization Code for Three-Dimensional Cellular Materials Written in Matlab”. In: *Journal of Engineering Materials and Technology* 141.1 (July 2018), p. 011005.

- [13] Federico Ferrari and Ole Sigmund. “A New Generation 99 Line MATLAB Code for Compliance Topology Optimization and Its Extension to 3D”. In: *Struct. Multidiscip. Optim.* 62.4 (Oct. 2020), pp. 2211–2228.
- [14] Oliver Giraldo-Londoño and Glaucio H Paulino. “PolyStress: a Matlab implementation for local stress-constrained topology optimization using the augmented Lagrangian method”. In: *Struct. Multidiscip. Optim.* 63.4 (Apr. 2021), pp. 2065–2097.
- [15] J. Lógó. “New Type of Optimality Criteria Method in Case of Probabilistic Loading Conditions”. In: *Mechanics Based Design of Structures and Machines* 35.2 (2007), pp. 147–162.
- [16] János Lógó. “SIMP type topology optimization procedure considering uncertain load position”. In: *Periodica Polytechnica Civil Engineering* 56 (2012), pp. 213–219.
- [17] János Lógó, Mohsen Ghaemi, and Majid Movahedi Rad. “Optimal Topologies in Case of Probabilistic Loading: The Influence of Load Correlation”. In: *Mechanics Based Design of Structures and Machines* 37.3 (2009), pp. 327–348.
- [18] János Lógó, Mohsen Ghaemi, and Anna Vásárhelyi. “Stochastic compliance constrained topology optimization based on optimality criteria method”. In: *Periodica Polytechnica Civil Engineering* 51.2 (2007), pp. 5–10.
- [19] Erika Pintér, András Lengyel, and János Lógó. “Structural topology optimization with stress constraint considering loading uncertainties”. In: *Period. Poly. Civ. Eng.* 59.4 (2015), pp. 559–565.
- [20] A. Prékopa. *Stochastic Programming*. Budapest, Dordrecht: Akadémia Kiadó and Kluwer, 1995.
- [21] Marcos Valdebenito and Gerhart Schuëller. “A survey on approaches for reliability-based optimization”. In: *Structural and Multidisciplinary Optimization* 42 (Nov. 2010), pp. 645–663.
- [22] Jun Wu, Ole Sigmund, and Jeroen P. Groen. “Topology optimization of multi-scale structures: a review”. In: *Structural and Multidisciplinary Optimization* 63 (2021), pp. 1455–1480.
- [23] Konstantinos-Iason Ypsilantis, Georgios Kazakis, and Nikos Lagaros. “An efficient 3D homogenization-based topology optimization methodology”. In: *Computational Mechanics* 67 (Feb. 2021), pp. 481–496.